Steady-State Convection and Fluctuation-Driven Particle Transport in the *H*-Mode Transition

G. R. Tynan, L. Schmitz, R. W. Conn, R. Doerner, and R. Lehmer

Institute for Plasma and Fusion Research, University of California, Los Angeles, California 90024

(Received 21 November 1991)

Large-scale steady-state convection is found to dominate the particle transport just inside the last closed flux surface (LCFS) in Ohmic discharges in the CCT tokamak. Near the limiter radius and in the scrape-off layer, fluctuation-induced transport is prevalent. At the *L-H* transition, the convection pattern near the LCFS is disrupted and a more poloidally symmetric, near-sonic plasma flow develops. Convective and turbulent particle transport are reduced across the entire edge region, resulting in the formation of the *H*-mode edge transport barrier.

PACS numbers: 52.25.Fi, 52.35.Ra, 52.55.Fa, 52.55.Pi

Results from a number of tokamak experiments have clearly demonstrated a degradation of energy and particle confinement with increasing auxiliary heating power [1]. This behavior, referred to as "*L*-mode" scaling, makes the achievement of a burning fusion plasma more difficult. The experimental observation of a regime with improved energy and particle confinement (the "*H*-mode" regime), first in ASDEX [2] and subsequently in other tokamaks [3], is thus significant. Recent measurements in Doublet III-D indicate that a localized radial electric field develops just inside the last closed flux surface (LCFS) at the *L-H* transition [4] and that the density fluctuation amplitude is reduced [5].

Electrostatic edge turbulence has been shown to be an important transport mechanism in Ohmic plasmas in the TEXT tokamak [6] and during auxiliary heating in ISX-*B* and DITE [7,8]. It has been suggested that sheared poloidal plasma flow may locally decorrelate the turbulent fluctuations and thereby reduce the associated particle transport [9]. A transport barrier would then be created in the region of strongly sheared rotational flow. Here, we present experimental evidence that the edge turbulence and the associated particle transport are modified across the entire edge plasma region in the *H* mode. Furthermore, it is shown that large-scale steady-state $\mathbf{E}\times\mathbf{B}$ convection (observed in several devices [10–12] but often thought to be small or neglected [6]) is also an important transport mechanism in CCT during the Ohmic *L* mode. The radial component of this convective flow across the LCFS is substantially reduced during the *H*-mode phase, providing a second mechanism for the formation of an edge plasma transport barrier.

The results presented in this paper are obtained at a magnetic field of 0.25 T ($q_a \approx 3$) with a total plasma current of 38 kA, a line-averaged density of $n = 3\times10^{12}$ cm^{-3}, a loop voltage of 1.4 V, and plasma major and minor radii of 148 and 36 cm, respectively. The inside midplane of the conducting vacuum chamber liner is used as the limiter, and the gap between the LCFS and the outside midplane wall is 4 cm. The plasma position is controlled to within 0.5 cm by means of a fast response feedback system.

A poloidal Langmuir probe array with 15° poloidal spacing between probes is used to measure the equilibrium plasma profiles, the steady-state convective transport, and the turbulence-induced transport over the region 30° above and below the outside midplane. Each probe assembly (diameter $d_p = 0.5$ cm) has two tips measuring the floating potential fluctuations at two closely spaced poloidal positions ($d = 0.3$ cm). A third tip, located on the same field line as one of the floating tips, is biased to ion saturation current to measure the ion density fluctuations. The fourth probe tip is used as a swept Langmuir probe.

A biased electrode, inserted to $r/a \approx 0.75$ (here a is the plasma minor radius) at a poloidal angle $\theta = 90°$ above the outside midplane and a toroidal separation of 105° from the probe array, is used to induce the CCT *H* mode

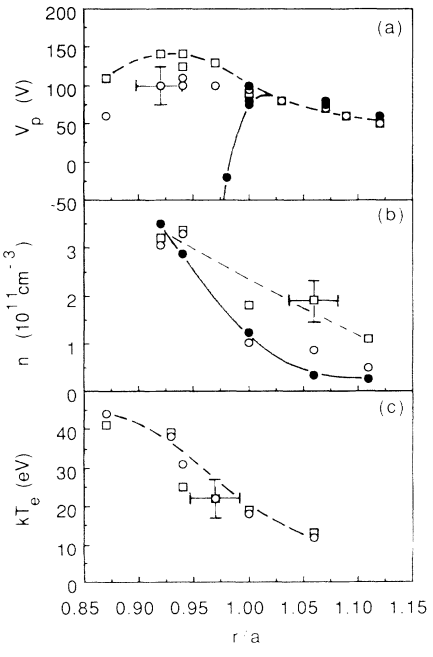

FIG. 1. (a) Plasma potential, (b) equilibrium density, and (c) electron temperature profiles on the outside midplane region during Ohmic *L*-mode phase (□), with injected current on but prior to bifurcation (○), and during the *H*-mode confinement regime (●). The density profile steepens and a strong radially inward electric field develops during the *H*-mode transition.

[13]. Over a 15-ms period, the electrode is biased by an external power supply to -250 V with respect to the vacuum vessel to study the evolution of the edge plasma transport during the L-H transition. Electron injection by the electrode causes a radial current of up to 20 A to flow to the wall. At a critical value of injected current, the plasma bifurcates to a new equilibrium characterized by a strong radially inward electric field $E_r \approx -100$ V/cm just inside the LCFS and an increased global particle confinement time [13]. No significant changes in the plasma current and the loop voltage are observed.

The plasma potential profile $V_p(r)$ is calculated from the measured floating potential and electron temperature profiles [14]. During the Ohmic L-mode phase of the discharge, the plasma potential profile is peaked 1–2 cm inside the LCFS [see Fig. 1(a)], as seen in other tokamaks [15]. Beyond this peak, there is a radially outward electric field, $E_r \approx 10$ V/cm, while radially inward of this peak, $E_r \approx -10$ V/cm. The total time-stationary electric field $\mathbf{E}$ causes the plasma to drift at a velocity given by $\mathbf{v}_E = \mathbf{E} \times \mathbf{B}/B^2$. Typically $v_{E_r} \approx 5 v_D$ in an Ohmic discharge (here v_D is the electron diamagnetic drift speed) and hence $\mathbf{v}_E$ provides an adequate description of the guiding-center dynamics. During the H mode the peak in $V_p(r)$ moves out to the LCFS, E_r becomes more negative, and v_{E_r} approaches a value of $0.6 c_s$, where c_s is the ion acoustic speed (as shown by an increased poloidal fluctuation phase velocity).

The edge density profile $n(r)$ steepens in the H mode [see Fig. 1(b)] while the electron temperature profile $T_e(r)$ is unchanged [see Fig. 1(c)]. Much larger increases in $\nabla_r n$ occur when the fueling rate is held constant [13]. Here the line-averaged density is held constant by reducing the neutral-gas feed rate by a factor of 3–5 in the H mode. The net plasma fueling rate is then reduced by a corresponding factor, indicating that the global particle confinement time has increased (the recycling coefficient of the titanium gettered wall is unchanged in the transition, and ionization sources are much smaller than $\nabla_\perp \cdot \Gamma$ and $\nabla_\parallel \cdot \Gamma$ at the edge). The steepened density gradient, coincident with the strong radial electric field, then implies the formation of an edge transport barrier near the LCFS [13].

The plasma potential varies in the poloidal direction in CCT Ohmic discharges, resulting in a spatially varying poloidal electric field E_θ of 10 to 20 V/cm. The top panels of Fig. 2 show the evolution of $\mathbf{v}_E(r,\theta)$ inferred from the measured $\mathbf{E}(r,\theta)$ during the L-H transition, with $\mathbf{E}(r,\theta)$ measured on a 0.3-cm spatial scale poloidally and on a 1-cm scale radially. Large-scale, steady-state convection patterns ($L_r \approx 2$–3 cm and $L_\theta \approx 20$–30 cm) are observed during the Ohmic L mode. Before the

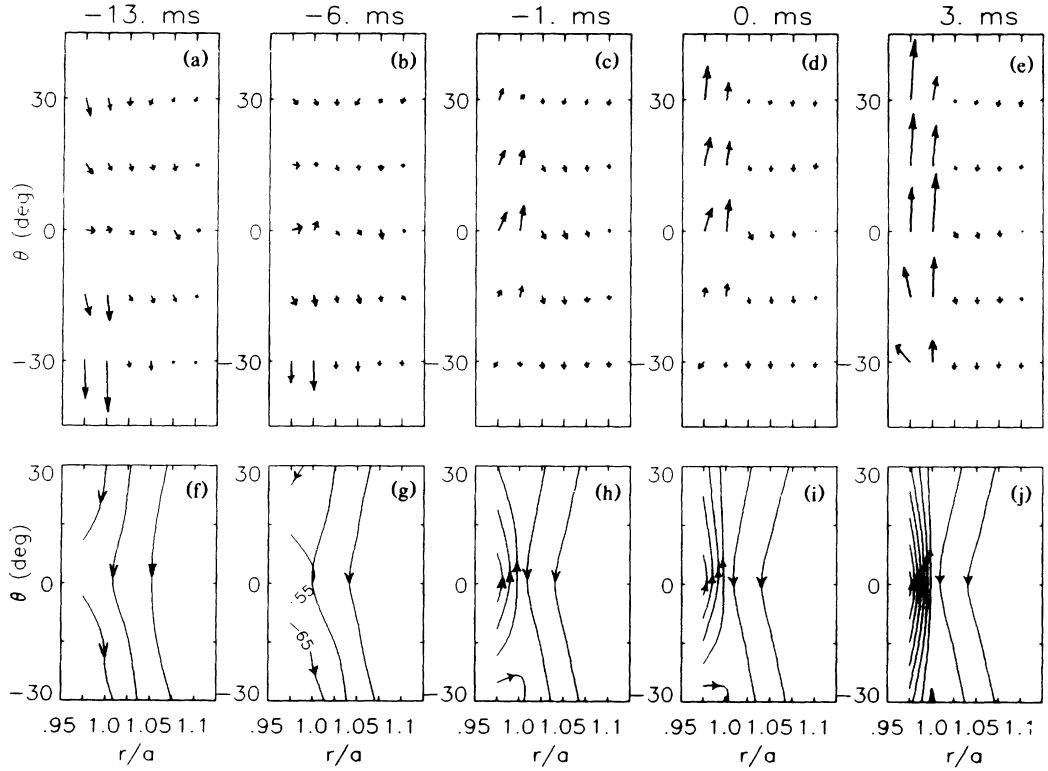

FIG. 2. Top panels (a)–(e) show the evolution of the convective velocity $\mathbf{v}_E(r,\theta)$ during the CCT L-H transition. The lower panels (f)–(j) show the evolution of the plasma potential distribution $V_p(r,\theta)$ during the L-H transition. During the Ohmic L mode (-13 ms), a large-scale eddy pattern exists at the plasma edge and causes significant radial transport. The eddy pattern is gradually modified as the injected current is increased (-6 to -1 ms). At bifurcation (0 ms) a strong poloidal flow develops.

current is injected, the plasma flows in the ion-diamagnetic direction in the scrape-off-layer (SOL) region and flows in the electron drift direction inside $r/a \approx 1.0$. The flow also has significant radial components (10^5 cm/s $\leq v_{E_r} \leq 10^6$ cm/s), causing radial particle transport inside of and across the LCFS.

There are several possible explanations for the observed large-scale convection pattern. A magnetic error field of order $\delta B_r/B \approx 10^{-3}$ can produce magnetic islands of radial width $L_r \approx 5$ cm [16], and in turn produce convective cells of a similar scale size. Measurements in L-mode plasmas with a slowly ramped plasma current show that the convective flow profile at the outside midplane depends upon q_a, suggestive of such islands. During the Ohmic L mode, the CCT edge plasma is marginally unstable to the transverse Kelvin-Helmholtz (K-H) mode [17]. The antisymmetric $E_r(r)$ profile in the L mode [see Fig. 1(a)] and the associated poloidal flow profile might then excite a stationary vortex pattern, as observed in particle simulations [18]. A K-H instability may be less likely during the H mode due to finite-Larmor-radius effects produced by the close vicinity of the two shear flow layers.

The convective flow near the LCFS is gradually modified as the injected electron current is increased and the L-H transition is approached. As the inward radial electric field becomes strong enough, a flow reversal occurs near the LCFS [see Figs. 2(b)–2(d)]. After the L-H transition [see Fig. 2(e)], a near-sonic poloidal plasma flow parallel to the electron diamagnetic drift direction is observed. The radial component of $\mathbf{v}_E$ is decreased by a factor of 3–5 during the H mode, indicating the reduction of radial convection across the LCFS.

The temporal evolution of $V_p(r,\theta)$ as measured on a large (10 cm) poloidal scale and a narrow (1 cm) radial scale is depicted in Figs. 2(f)–2(j). In the Ohmic L mode, an X point in the flow distribution is observed slightly above the outside midplane at $r/a \approx 0.95$, suggesting the presence of a large-scale eddy at the plasma edge. As the transition to the H mode occurs, the X point first moves out to $r/a = 1.0$ [Fig. 2(g)] and then moves downwards. After the bifurcation, the X point disappears and a uniform poloidal plasma flow develops that is characteristic of the H mode.

The edge plasma turbulence also exhibits a number of changes during the L-H transition. The strong radial electric field causes a large Doppler shift in the average frequency (by more than a factor of 5) of the fluctuating density and potential. The absolute density fluctuation level is reduced from the electric field layer out to the wall [see Figs. 3(a) and 3(b)]. However, the equilibrium density is also reduced across this region as noted earlier. As a result, the normalized density fluctuation level $\tilde{n}/\langle n\rangle$ is nearly unchanged near the radial electric field layer [see Fig. 3(c)]. The poloidal electric field fluctuation level, however, is reduced substantially across the entire edge region [see Fig. 3(d)]. The radial turbulent particle flux $\tilde{\Gamma}_r$ and the radial turbulent drift speed $\tilde{\Gamma}_r/\langle n\rangle$ are also both reduced across the entire edge region as the rotation rate is increased [see Figs. 3(e) and 3(f)]. Both $\tilde{\Gamma}_r$ and $\tilde{\Gamma}_r/\langle n\rangle$ are reduced by a factor of 3–5 from the values

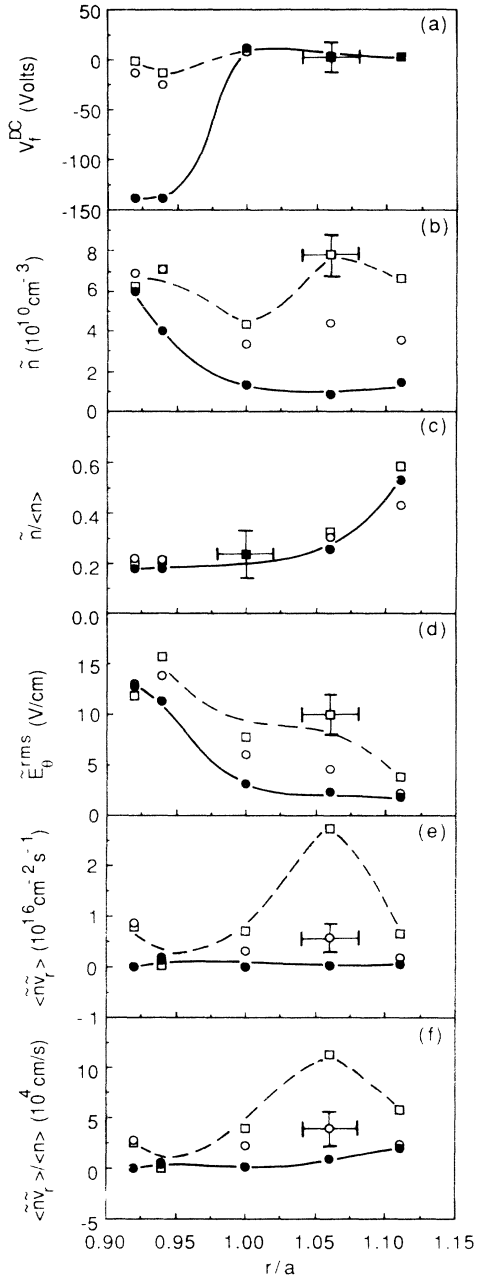

FIG. 3. Turbulence levels and transport in the CCT edge and SOL plasma in the Ohmic L mode (□), with biasing but before bifurcation (○), and during the H mode (●): (a) dc floating potential profiles; (b) absolute ion saturation current fluctuation levels; (c) normalized ion saturation current fluctuation levels; (d) fluctuating poloidal electric field levels; (e) radial turbulent particle flux; and (f) radial turbulent drift speed. During the L-H transition, significant changes in $\tilde{E}_\theta$, $\langle\tilde{n}\tilde{v}_r\rangle$, and $\langle\tilde{n}\tilde{v}_r\rangle/\langle n\rangle$ occur across the entire edge region.

found during the Ohmic phase. The changes in the turbulence are not localized to the narrow region where the strong radial electric field or sheared rotation occur, as observed in TEXT [19].

During the Ohmic confinement phase, the time for electrostatic turbulence to transport plasma across the edge density gradient can be estimated as $\tau_{fl} \approx \langle n \rangle L_n / \tilde{\Gamma}_r \approx 200$ μs, where L_n is the edge density gradient scale length. The parallel transit time is $\tau_{\parallel} \approx qR/c_s \approx 200$ μs, where q is the safety factor and R is the major radius. The turnover time of the large-scale eddy pattern seen during the Ohmic regime is estimated as $\tau_{rot} \approx L_{\perp} / \langle v_E \rangle \approx 200$ μs, where $L_{\perp}$ is the circumference of the eddy and $\langle v_E \rangle$ is the eddy rotation speed. The time for the plasma to complete one poloidal rotation is $\tau_{\theta} \approx 2\pi a / \langle v_{E_r} \rangle \approx 400$ μs. Hence during the Ohmic confinement phase, $\tau_{fl} \approx \tau_{\parallel} \approx \tau_{rot} < \tau_{\theta}$. The rapid radial transport of plasma can then overcome parallel equilibration flows, allowing significant pressure variations to occur on a magnetic flux surface (along with corresponding parallel reconnecting flows) [20], and should lead to significant poloidal transport asymmetries [21].

In the H mode, $\tau_{\theta} \approx 50$ μs in the region of strong poloidal plasma flow. The fluctuation-driven transport is reduced and hence τ_{fl} is increased ($\tau_{fl}^{H} > 1$ ms). The parallel transit time $\tau_{\parallel}$ is unchanged from the Ohmic value. The shear decorrelation time for the large-scale eddy pattern is estimated as $\tau_{shear} \sim L_{\theta} L_v / v_{\theta} L_r \sim 5$ μs, where L_r and L_{θ} are the radial and poloidal scale lengths of the convection pattern and v_{θ} and L_v are the H-mode poloidal velocity and the velocity gradient scale length. Thus the rapid flow prohibits the formation of the slowly moving large-scale vortices (hence τ_{rot} is no longer a relevant time scale in the H mode). In the H mode, $\tau_{\theta} \ll \tau_{fl}, \tau_{\parallel}$ so that pressure variations on magnetic surfaces near the LCFS are eliminated by the poloidal plasma flow. The elimination of $\nabla_{\parallel} p$ implies that $v_{\parallel}$ is also reduced or eliminated in the H mode. As a result, the residual transport in the H mode should be nearly poloidally symmetric.

The authors wish to thank R. J. Taylor for many valuable discussions and his continuous support of this work. We also gratefully acknowledge the support of the scientific and technical staff of the UCLA tokamak laboratory. This work was supported by the U.S. Department of Energy under Contract No. DE-FG03-86ER-52134.

[1] R. J. Goldston, Plasma Phys. Controlled Fusion **26**, 87 (1984).
[2] F. Wagner *et al.*, Phys. Rev. Lett. **49**, 1408 (1982).
[3] K. H. Burrell *et al.*, Phys. Rev. Lett. **59**, 1432 (1987).
[4] R. J. Groebner, K. H. Burrell, and R. P. Seraydarian, Phys. Rev. Lett. **64**, 3015 (1990).
[5] E. J. Doyle *et al.*, Phys. Fluids B **3**, 2300 (1991).
[6] A. J. Wootton *et al.*, Phys. Fluids B **2**, 2879 (1990).
[7] G. A. Hallock, A. J. Wootton, and R. L. Hickok, Phys. Rev. Lett. **59**, 1301 (1987).
[8] P. Mantica, G. Vayakis, and J. Hugill, Nucl. Fusion **31**, 1649 (1991).
[9] H. Biglari, P. H. Diamond, and P. W. Terry, Phys. Fluids B **2**, 1 (1990).
[10] A. V. Nedospasov *et al.*, J. Nucl. Mater. **176-177**, 169 (1990).
[11] V. P. Budaev *et al.*, J. Nucl. Mater. **176-177**, 705 (1990).
[12] R. Moyer *et al.*, J. Nucl. Mater. **176-177**, 293 (1990).
[13] R. J. Taylor *et al.*, Phys. Rev. Lett. **63**, 2365 (1989).
[14] F. F. Chen, in *Plasma Diagnostic Techniques*, edited by R. H. Huddlestone and S. L. Leonard (Academic, New York, 1965).
[15] Ch. P. Ritz, R. D. Bengtson, S. J. Levinson, and E. J. Powers, Phys. Fluids **27**, 2956 (1984).
[16] R. B. White, in *Reviews of Plasma Physics*, edited by A. A. Galeev and R. N. Sudan (North-Holland, Amsterdam, 1983), p. 664.
[17] T. Chiueh *et al.*, Phys. Fluids **29**, 231 (1986).
[18] P. L. Pritchett and F. V. Coroniti, J. Geophys. Res. **89**, 168 (1984).
[19] Ch. P. Ritz, H. Lin, T. L. Rhodes, and A. J. Wootton, Phys. Rev. Lett. **65**, 2543 (1990).
[20] J. F. Drake, A. B. Hassam, P. N. Guzdar, and C. S. Liu, University of Maryland Report No. UMLPR 91-054, 1991 (to be published).
[21] G. R. Tynan, Ph.D. thesis, Institute of Plasma and Fusion Research, University of California, Los Angeles, Report No. UCLA-PPG-1369, 1991 (unpublished).